Biochemical and Biophysical Research Communications 435 (2013) 216–221

Contents lists available at SciVerse ScienceDirect

Biochemical and Biophysical Research Communications

journal homepage: www.elsevier.com/locate/ybbrc

Bacillus thuringiensis Cry4Ba toxin employs two receptor-binding loops for synergistic interactions with Cyt2Aa2

Chitsirin Lailak [a,1], Tararat Khaokhiew [b,1], Chamras Promptmas [a,*], Boonhiang Promdonkoy [c], Kusol Pootanakit [d], Chanan Angsuthanasombat [d,*]

[a] Department of Clinical Chemistry, Faculty of Medical Technology, Mahidol University, Bangkok-noi, Bangkok, Thailand
[b] Center of Medical Laboratory Services, Faculty of Medical Technology, Mahidol University, Bangkok-noi, Bangkok, Thailand
[c] National Center for Genetic Engineering and Biotechnology, National Science and Technology Development Agency, Pathumthani, Thailand
[d] Bacterial Protein Toxin Research Cluster, Institute of Molecular Biosciences, Mahidol University, Nakornpathom, Thailand

ARTICLE INFO

Article history:
Received 5 April 2013
Available online 7 May 2013

Keywords:
Bacillus thuringiensis
Cry toxins
Cyt toxins
Larvicidal restoration
Quartz crystal microbalance
Receptor-binding loops
Synergism

ABSTRACT

We previously demonstrated that co-expression in *Escherichia coli* of *Bacillus thuringiensis* (*Bt*) subsp. *israelensis* Cry4Ba and *Bt* subsp. *darmstadiensis* Cyt2Aa2 shows high synergistic toxicity against target mosquito larvae. Here, further insights into synergistic interactions between these two toxins were revealed through bioactivity restoration of particular inactive Cry4Ba-mutant toxins altered within the receptor-binding domain. Specific mutations at β2–β3 (Y332A) or β4–β5 (F364A) loops, but neither at three other β-hairpin loops (β6–β7, β8–β9 and β10–β11) of Cry4Ba, adversely affect toxicity restoration by Cyt2Aa2. Binding analysis using quartz crystal microbalance verified a decrease in binding of these two bioinactive-mutant toxins (Y332A and F364A) to the immobilized Cyt2Aa2. This suggests that Cry4Ba utilizes these two critical aromatic loop-residues, Tyr^{332} and Phe^{364}, for synergistic toxicity with its alternative receptor-Cyt2Aa2.

1. Introduction

Gram-positive, spore-forming *Bacillus thuringiensis* subsp. *israelensis* (*Bti*) produces insecticidal crystal inclusions comprising both crystalline (Cry) and cytolytic (Cyt) δ-endotoxins, *i.e.* Cry4Aa (134 kDa), Cry4Ba (128 kDa), Cry11Aa (65 kDa) and Cyt1Aa (27 kDa), which are specifically toxic to mosquito larvae [1–3]. Due to the efficacy and safety for non-target organisms of these crystal toxins, *Bti* has become one of the most promising biopesticides for the control of mosquito-carrying contagious diseases, including dengue-viral hemorrhagic fevers and malaria [2,4].

Dissimilar to the Cyt1Aa crystal structure which comprises a single α/β domain [5], the structures of the two closely related *Bti*-Cry4Aa and Cry4Ba mosquito-specific toxins reveal their overall structural features similar to that of several other known Cry toxins [3,6,7]. This suggests that the *Bt*-Cry toxins all share the same common mechanism of toxicity that is conceivably somewhat different from the toxic action of Cyt toxin family [1,3]. The Cry toxin structures show a wedge-shaped form with approximate dimensions of 55 × 65 × 75 Å and consist of three structurally and functionally distinctive domains (I–III) [3,6–8]. The N-terminal α-helical bundle (domain I) and the β-sheet prism (domain II) have been revealed to be membrane pore-forming and receptor-binding domains, respectively [3,6–8]. Thus far, nearly all studies regarding receptor-binding of β-hairpin loops composing of Cry-domain II are still restricted to the three loops connecting β2–β3, β6–β7 and β10–β11 which were assigned as loops 1, 2 and 3, respectively [8]. Nevertheless, we have shown that two other β-hairpin loops of β4–β5 and β8–β9 within the receptor-binding domain are also involved in receptor recognition [9,10].

Synergistic combinations of *Bti*-Cry and Cyt toxins have been demonstrated to be much more toxic than each individual against mosquito larvae [11–14]. For instance, Cyt1Aa has been reported to play a key role in synergistic actions with Cry4Aa, Cry4Ba or Cry11Aa for delaying the development of resistance to these toxins in *Culex* larvae [13,14]. Thus, Cyt1Aa has been proposed to serve as a functional receptor for promoting the binding of *Bti*-Cry toxins to target membranes [15]. In our earlier studies, co-expression in *Escherichia coli* of *Bti*-Cry4Ba and Cyt2Aa2 from *Bt* subsp. *darmstadiensis* (*Btd*) was found to be synergistically active against mosquito larvae, albiet no verification yet on their synergistic interactions [16]. Here, in an effort to provide further insights into the detailed synergistic interactions between these two toxins, we

* Corresponding authors.
E-mail addresses: chamras.pro@mahidol.ac.th (C. Promptmas), chanan.ang@mahidol.ac.th (C. Angsuthanasombat).
[1] These authors equaly contributed to this work.

0006-291X/$ - see front matter © 2013 Elsevier Inc. All rights reserved.
http://dx.doi.org/10.1016/j.bbrc.2013.04.078

have assessed potential restoration of larvicidal activity by *Btd*-Cyt2Aa2 of several inactive Cry4Ba-mutant toxins mutated either in the pore-forming domain or in all five β-hairpin loops composing the receptor-binding domain. Our data suggest that Cry4Ba specifically employs two receptor-binding loops, *i.e.* β2–β3 and β4–β5 loops, in binding with its alternative receptor-Cyt2Aa2 for synergistic toxicity against target mosquito larvae.

2. Materials and methods

2.1. Construction of Cry4Ba mutant plasmids

pMU388 plasmid encoding the 130-kDa *Bti*-Cry4Ba toxin under control of the *lac* promoter [17] was used as a template. Complementary pairs of mutagenic oligonucleotide primers (*see* Supplementary Table 1) were designed according to the sequence of the *cry4Ba* gene to generate mutant plasmids using a high fidelity *Pfu* DNA polymerase (Promega, USA), following the PCR-based QuickChange Mutagenesis procedure (Stratagene, USA). The *Dpn*I-treated PCR products were transformed into *E. coli* strain JM109. The selected clones were subjected to restriction endonuclease analysis and subsequently verified by DNA sequencing (Macrogen, Inc., Korea).

2.2. Expression and purification Cry4Ba and Cyt2Aa toxin inclusions

After 4-h induction with isopropyl-β-D-thiogalactopyranoside (0.1 mM final concentration), the toxins were overexpressed in *E. coli* JM109 grown at 37 °C in Luria–Bertani broth containing ampicillin (100 μg/mL). The expressed target toxins were analyzed by SDS–PAGE (sodium dodecyl sulfate–polyacrylamide gel electrophoresis). Cells expressing each individual protoxin as inclusions were disrupted by using a French Pressure Cell (10,000 psi) and the inclusions were partially purified from crude lysate by centrifugation (6000*g* for 10 min at 4 °C).

2.3. Preparation of Cry4Ba and Cyt2Aa activated toxins

For toxin activation, the protoxin inclusions of Cry4Ba and Cyt2Aa2 were first solubilized in carbonate buffer (50 mM Na_2CO_3/$NaHCO_3$, pH 10.0) at 5 mg/mL final concentration for 1 h at 37 °C. Subsequently, the solubilized Cry4Ba protoxin was treated with trypsin (tolylsulfonyl phenylalanyl chloromethyl ketone-treated; Sigma) at a ratio of 1:20 (w/w) for 16 h at 37 °C, while the Cyt2Aa2 protoxin was activated by digesting with chymotrypsin at a ratio of 1:50 enzyme/toxin (w/w) for 2 h at 37 °C in the carbonate buffer (pH 10.0).

The activated toxins were further purified using a size-exclusion FPLC system (Superose 12 column; GE Healthcare Life Biosciences) eluted with the carbonate buffer (pH 10.0) at a flow rate of 0.4 mL/min. Protein concentrations of the purified toxins were determined using the Bradford-based protein microassay (Bio-Rad), with bovine serum albumin (BSA fraction V, Sigma) as a standard protein, and were subsequently analyzed by SDS–PAGE.

2.4. In situ binding assays via immunohistochemical staining

Sections of paraffin-embedded tissues were prepared from 5-day-old *Aedes aegypti* larvae and immunohistochemical staining was carried out following the method described previously [18]. In detection assays, FPLC-purified toxins (12.5 mg/mL) were used, and sequentially probed with the 2F-1H2 anti-Cry4Ba-domain III monoclonal antibody [19] (1:50 dilution), biotin-conjugated rabbit anti-mouse IgGs (1:8000 dilution) and peroxidase-conjugated streptavidin (1:50,000 dilution). Finally, color development was done with a 3,3′-diaminobenzidine solution (SK-4100, Vector).

2.5. Bioactivity restoration assays

Larvicidal activity of Cyt2Aa2 and Cry4Ba or its mutants (individuals and combination) was evaluated against 2-day old *A. aegypti* larvae. The assays were carried out in 24-well polystyrene plates (1.5-cm well diameter, Costar) with 2 mL/well of *E. coli* suspension ($\sim 10^7$ cells). 100 larvae (10 larvae/replicate × 10 replicates) were fed with different ratios and concentrations of toxin-expressing *E. coli* suspension. The cells containing each individual corresponding vector, pUC12 and pBC* [16] were used as negative controls for Cry4Ba and Cyt2Aa2, respectively. Mortalities were recorded after 24-h treatment at room temperature (~25 °C).

2.6. Binding analysis via quartz crystal microbalance (QCM)

QCM-based biosensor was performed using a research quartz crystal microbalance (RQCM, Maxtek Inc.) with gold-plated 9 MHz AT-cut QCM crystals (25 mm diameter, 185 μm thickness; 137 mm^2 front electrode area). Surface contaminants were removed by immersing the crystals in a freshly prepared Piranha solution (3:1 mixture of 98% H_2SO_4 and 30% H_2O_2) for 1 min at room temperature, followed by a thorough rinse with distilled water, then ethanol, and finally drying under a gentle N_2 stream. Subsequent to the cleaning process, the front gold-electrode was immediately coated with 10 mM MPA (mercaptopropionic acid) at room temperature in a moisture chamber for at least 1 h. After rinsing with ethanol, distilled water and drying under a N_2 stream, the carboxyl groups of the deposited MPA-monolayer on the electrode surface were then converted to amine reactive by activating with 200 mM EDC (1-ethyl-3-(3′-dimethylaminopropyl)-carbodiimide and 50 mM NHS (*N*-hydroxysuccinimide) in 10 mM HEPES buffer (pH 7.5) for 30 min at room temperature. An excess EDC/NHS was removed by washing with distilled water repeatedly.

For toxin immobilization, 500 μL of the Cyt2Aa2 activated toxin (10 μg/mL, ~0.4 μM) was covalently linked to the amine-reactive surface of the activated sensor placed in the RQCM cell holder containing 10 mM HEPES buffer (pH 7.5) and 100 mM NaCl. The residual reacting sites were deactivated with 1 mM ethanolamine for 20 min, and the remaining ethanolamine was removed by flowing with HEPES buffer for 5 min. For binding analysis, the trypsin-treated toxin of either Cry4Ba or its mutants (50 μg/mL) was injected onto the Cyt2Aa2-immobilized sensor surface and incubated for 1 h. Data recorded on a desktop PC using the Maxtek RQCM logging software at a rate of 10 data points/min. Frequency responses (ΔF) in the QCM sensorgram were measured in Hz, as ascribed to the mass increase from Cry4Ba binding to CrytAa2 on the sensor surface in accordance with a Sauerbrey sensitivity factor (Cf) of 6.217 ng/Hz.

3. Results and discussion

3.1. Biochemical and functional characterization of the expressed Cry4Ba-loop mutants

Based on its crystal structure, the mosquito-specific Cry4Ba toxin contains five β-hairpin loops of β2–β3, β4–β5, β6–β7, β8–β9 and β10–β11 composing the receptor-binding domain (Fig. 1A). We have previously employed PCR-based mutagenesis and demonstrated that several residues within the loops linking β6–β7, (Pro^{389}) β8–β9 (Glu^{417}) and β10–β11 (Tyr^{455}) are critically involved in receptor binding and toxicity of this mosquito-specific toxin (9,10; *see* Fig. 1A). In this study, we have applied the same muta-

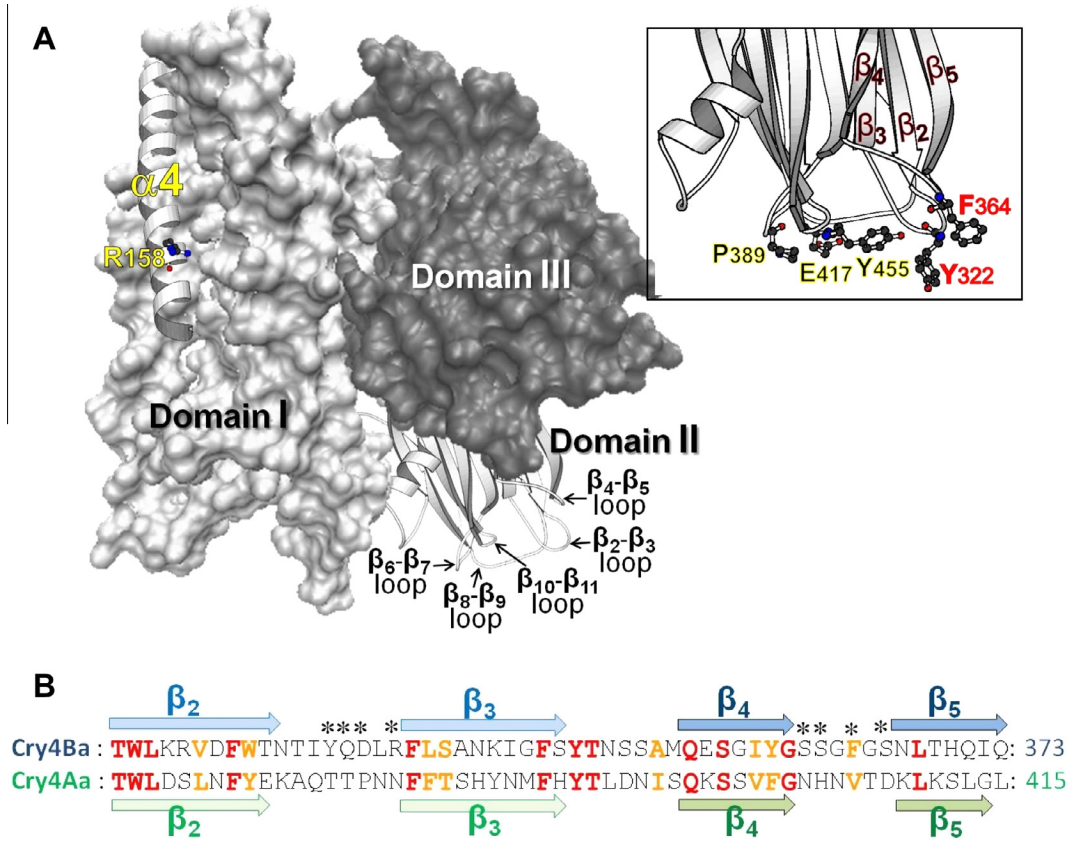

Fig. 1. (A) The three-domain Cry4Ba structure [6] illustrating five β-hairpin loops composing the receptor-binding domain (domain II, schematic ribbon). Helix 4 (schematic ribbon) within domain I (space-filling) shows the location of Arg^{158} (ball-and-stick). Inset, five critical residues in domain II; Tyr^{332} (β2–β3 loop), Phe^{364} (β4–β5 loop), Pro^{389} (β6–β7 loop), Glu^{417} (β8–β9 loop) and Tyr^{455} (β10–β11 loop), are shown in ball-and-stick representations. The structure was generated by using MOLSCRIPT and VMD programs. (B) Sequence alignments of two β-hairpins (β2–β3 and β4–β5) of Cry4Ba with those of its closely related Cry4Aa structure [7]. Corresponding β-strands of Cry4Ba and Cry4Aa are illustrated over and under the sequences, respectively. Mutated residues (Tyr^{332}, Gln^{333}, Asp^{334}, Arg^{336}, Ser^{361}, Ser^{362}, Phe^{364} and Ser^{366}) are indicated by *.

genic strategy to further investigate a possible involvement in receptor binding of residues within two other loops of β2–β3 and β4–β5. Total eight selected residues in β2–β3 (Tyr^{332}, Gln^{333}, Asp^{334} and Arg^{336}) and β4–β5 (Ser^{361}, Ser^{362}, Phe^{364} and Ser^{366}) were initially mutated to alanine (see Fig. 1B). When each mutant toxin was expressed in *E. coli* upon IPTG induction, all were produced as inclusion bodies, and the expression levels of the 130-kDa mutant protoxins was comparable to that of the wild-type toxin (*see* Supplementary Fig. 1A). It has long been known that the 130-kDa Cry4Ba protoxin is cleaved by trypsin into two major protease-resistant fragments of ~47 and ~20 kDa, in addition to the deletion of the C-terminal half of the protoxin [20]. Here, we also examined for trypsin-digesting susceptibility of the mutant protoxins which can be solubilized in the carbonate buffer (pH 10.0). All the 130-kDa soluble mutant toxins were found to yield the 47- and 20- kDa trypsin-resistant fragments that are the same for the products produced from the wild-type protoxin (*see* Supplementary Fig. 1B), signifying that all these mutants were produced as structurally stable protoxins and that the mutations had no apparent adverse effects on proteolytic activation of the solubilized mutant toxins.

To determine a consequence of these single-alanine substitutions, *E. coli* cells expressing each mutant toxin were assayed for their relative biological activity against *A. aegypti* larvae. The mortality data revealed that only the Y332A and F364A mutants showed a drastic decrease in larvicidal activity, while six other mutants (Q333A, D334A, R336A, S361A, S362A and S366A) still exhibited high toxicity similar to the wild-type toxin (Fig. 2A). These results suggested that Tyr^{332} and Phe^{364} in β2–β3 and β4–β5 loops, respectively, play an important role in Cry4Ba toxicity. Further replacement of Tyr^{332} and Phe^{364} with an aromatic side-chain (*i.e.* Y332F, F364Y and F364W), did not affect the toxicity (*see* Fig. 2A, shaded graphs). These results revealed a crucial role in the Cry4Ba toxin activity for the conserved aromatic residue at both apex positions of β2–β3 and β4–β5 loops. In addition, *in situ* binding analysis was performed to determine whether the loss of toxicity of these two loop-mutant toxins (Y332A and F364A) is associated with their inefficiency in binding to the target receptors. The results revealed that the purified trypsin-activated proteins of both loop-mutant toxins exhibited a marked decrease in the immunochemical signal detected on the apical-brush border of posterior midgut sections (Fig. 2B), further suggesting that these two loop-residues (Tyr^{332} and Phe^{364}) play a crucial part in receptor-binding activity of the Cry4Ba toxin.

3.2. Bioactivity restoration of inactive Cry4Ba-mutants by Cyt2Aa2

Our previous studies on co-expression in *E. coli* of *Bti*-Cry4Ba and *Btd*-Cyt2Aa2 provided evidence for synergistic toxicity of these two toxins against target mosquito larvae, although there is no confirmation yet on their synergistic interactions [16]. In this regard, we therefore performed bioassays against *A. aegypti* larvae to test if there is toxicity restoration by Cyt2Aa2 of various selected inactive-Cry4Ba mutant toxins. Bioactivity data of individual toxin-producing *E. coli* cells that were fed singly compared with that from assaying the cell mixtures revealed that the mixture of Cyt2Aa2 and wild-type Cry4Ba (ratio 1:40; 2.5×10^6:2.5×10^7 cells/mL) was much more toxic than Cry4Ba alone, giving >90% larval

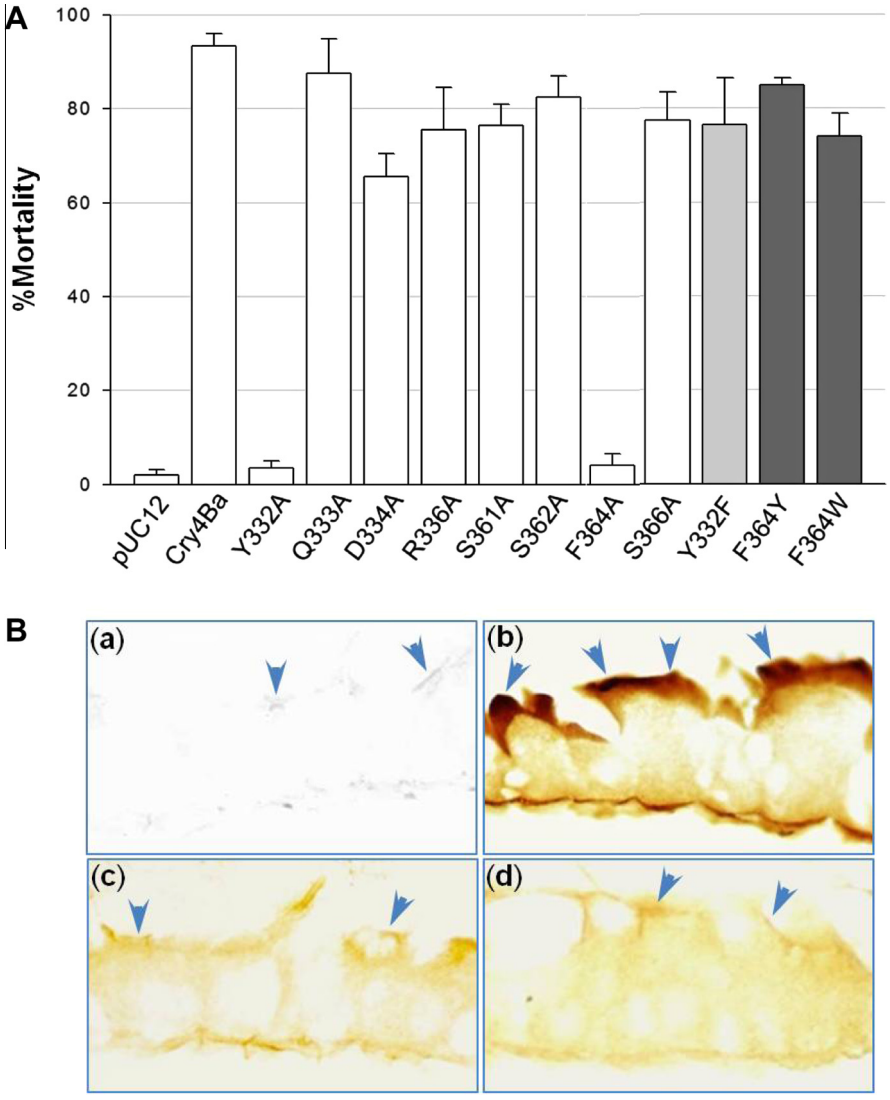

Fig. 2. (A) Larvicidal activities of *E. coli* cells (~10^8 cells/mL) expressing the Cry4Ba wild-type or its mutant toxins against *A. aegypti* larvae. Error bars indicate standard errors of the mean (SEM) from three independent experiments. Shaded graphs represent the larvicidal activity of the mutants of which Tyr^{332} or Phe^{364} were replaced with an aromatic side-chain. (B) Immuno-histochemical staining of 5-day-old *A. aegypti* larval midgut sections. Slides were incubated with either (b) the purified Cry4Ba wild-type toxin, (c) Y332A or (d) F364A mutant toxins. (a) Control slide omitting the tested proteins. Arrows indicate apical microvilli.

mortality as a result of synergism between these two toxins (Fig. 3B). Noteworthy that Cyt2Aa2-producing cells at a sub-lethal concentration of 2.5×10^6 cells/mL (equivalent to ~0.1 μg/mL) are insufficient to exert *in vivo* cytotoxicity (contributing <5% mortality). It should also be noted that all Cry4Ba mutant toxins were highly produced as 130-kDa protoxins at levels similar to the wild-type (*see* Fig. 3A). The larvae tested in the bioassays were hence considered to receive a comparable amount of the toxin doses.

Functional correlations between Cry4Ba and Cyt2Aa2 were further revealed when chosen larvicidal-inactive Cry4Ba mutants (2.5×10^7 cells/mL) were individually evaluated with Cyt2Aa2 at its sub-lethal concentration. Interestingly, mixtures of Cyt2Aa2 and Cry4Ba-mutant toxins of which are dually mutated at the receptor-binding loops at β6–β7 and β8–β9 (P389A/E417A) or at β8–β9 and β10–β11 (E417A/Y455A) showed high larvicidal activity as good as the mixture of Cyt2Aa2 and Cry4Ba wild-type (*see* Fig 3B), indicating that Cyt2Aa2 is able to restore the toxicity of both double-point mutants. This could suggest that these inactive Cry4Ba mutants act together somehow with Cyt2Aa2 for the recovery of their defective larvicidal activity. Conversely, it was revealed that Cyt2Aa2 was unable to restore larvicidal activity of neither two other Cry4Ba-loop mutants as identified above, *i.e.* Y332A and F364A which were mutated at β2–β3 and β4–β5 loops, respectively, suggesting that these two loops would play an important role in Cyt2Aa2–Cry4Ba interactions for restoring toxicity. As discussed earlier that aromaticity at both apex positions (*i.e.* Tyr^{332} in β2–β3 loop and Phe^{364} in β4–β5 loop, *see* Fig. 1A, inset) could be implicated in receptor-binding activity of the Cry4Ba toxin. This might put forward that Cry4Ba could employ both critical aromatic loop-residues (Tyr^{332} and Phe^{364}), but not other receptor-binding residues at three other β-hairpin loops (β6–β7, β8–β9 and β10–β1), to interact with Cyt2Aa2 for bringing back their defective toxicity. Hence, Cyt2Aa2 could compensate for an alternative binding-site to the larvicidal-inactive Cry4Ba mutants which were not mutated at Tyr^{332} or Phe^{364}. This notion is strengthen by restoration results from the mixture of Cyt2Aa2 and the Cry4Ba-R158A pore-forming mutant that also revealed incapability of toxicity restoration of this pore-forming mutant by Cyt2Aa2. It is worth mentioning that Arg^{158} is located in α4 composing the Cry4Ba-pore-forming domain (*see* Fig. 1A), and hence alanine-substitution at this position would likely to disturb pore-forming function rather

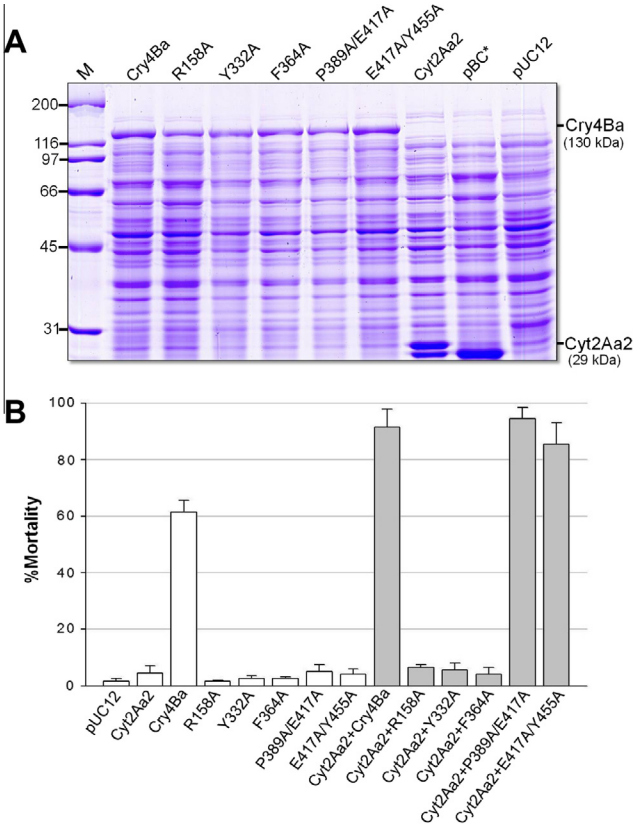

Fig. 3. (A) SDS–PAGE (Coomassie brilliant blue-stained 10% gel) of lysates extracted from *E. coli* (~10^7 cells) expressing Cry4Ba wild-type, its mutant toxins, or Cyt2Aa2. Cells harboring pUC12 or pBC* were used as negative controls for Cry4Ba and Cyt2Aa2, respectively. M, molecular mass standards. (B) Larvicidal activities of *E. coli* cells (~10^7 cells/mL) expressing Cyt2Aa2, Cry4Ba or its bio-inactive mutants. Shaded graphs are the bioactivity of the cell mixtures (Cyt2Aa with Cry4Ba or bio-inactive mutants). *E. coli* cells containing pUC12 were used as negative controls. Error bars show SEM over three independent experiments.

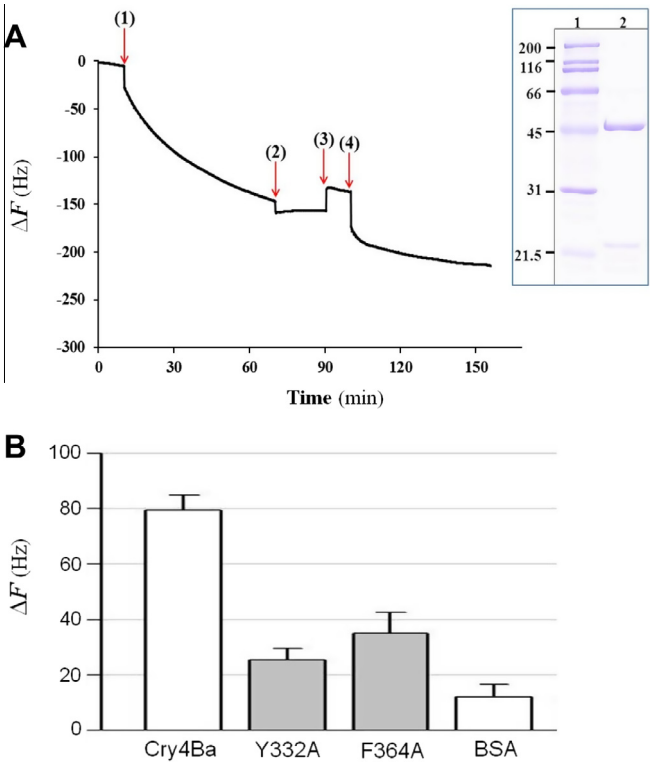

Fig. 4. (A) Typical sensogram of Cyt2Aa2-Cry4Ba interaction experiments. Normalized changes in resonant frequency (ΔF) at each of the measured overtones are plotted against time for pre-coating the QCM sensor cell with Cyt2Aa2 as well as subsequent Cry4Ba binding to the immobilized Cyt2Aa2. The introduction of (1) Cyt2Aa2 on a MPA-modified gold surface, (2) blocking buffer, (3) rinsing buffer, and (4) the purified activated Cry4Ba toxin are marked on the plot. Inset, the Cry4Ba toxin after trypsin activation, producing two non-covalently associated fragments of ~47 and ~20 kDa (lane 2). (B) Frequency shifts upon addition of Cry4Ba, its two critical aromatic-loop mutants (Y322A and F364A), or BSA (control) onto the sensor cell pre-coated with Cyt2Aa2. Error bars designate SEM over three independent experiments.

than toxin-receptor recognition [21]. Notwithstanding the lack of receptor-binding studies, the R158A mutant would still likely to bind to its natural receptors in *Aedes* larvae, but could not further exhibit bioactivity as it was perturbed in pore-forming capability. That is why Cyt2Aa2 was unable to restore the larvicidal activity of Cry4Ba-R158A despite the fact that its two important loop-residues (Tyr^{332} and Phe^{364}) are retained. Thus, it is reasonable to postulate that Cyt2Aa2 would assist Cry4Ba in receptor-binding phase rather than membrane insertion and pore formation, or conceivably serves as an alternative binding-site for Cry4Ba.

3.3. Binding analysis of Cry4Ba toxins to Cyt2Aa2-immobilized QCM

Attempts were further made to verify whether the adverse effects of the two specific mutations at β2–β3 (Y332A) or β4–β5 (F364A) loops on toxicity restoration by Cyt2Aa2 are associated with a decrease in their binding interactions. Binding analysis through the use of QCM technique has been recently established for binding studies of Cry4Ba to its counterpart receptor-alkaline phosphatase from *Aedes* larvae [22]. Here, when we then employed QCM-based biosensors to assess the interactions between the two bio-inactive Cry4Ba mutants (Y332A and F364A) and Cyt2Aa2, both mutants showed a marked reduction in their frequency shifts (ΔF ~30 Hz) as compared with the wild-type Cry4Ba (ΔF ~80 Hz) (*see* Fig. 4). This could indicate that Y332A and F364A mutants bind to the immobilized Cyt2Aa2 with lower affinity than does the wild type. Thus, these results further support an essential role of the two aromatic loop-residues (Tyr^{332} and Phe^{364} in β2–β3 and β4–β5 loops, respectively) in specific interactions with Cyt2Aa2 for toxicity restoration.

Previously, Pérez et al. demonstrated that two loops connecting α8–β1 and β10–β11 (assigned as loop α-8 and loop 3, respectively) of *Bti*-Cry11Aa are implicated in binding interactions with *Bti*-Cyt1Aa [23]. Additionally, Cantón et al. suggested that α8–β1 loop of Cry4Ba is involved in specific binding to Cyt1Aa for exhibiting synergism, as observed from a slight decrease in a calculated synergistic value of the mixture of Cyt1Aa and Cry4Ba-S303A/I304A which was dually mutated in α8–β1 loop but still retained high toxicity comparable to the wild-type toxin [24]. Dissimilar to our present findings as demonstrated above, Cry4Ba would rather utilize two β-hairpin loops of β2–β3 and β4–β5 for synergistic interacting with *Btd*-Cyt2Aa2 as their synergistic combinations have also been revealed previously [16]. Hence, our results together with that of other workers imply that individual Cry toxins, *e.g.* Cry4Ba and Cry11Aa, could perhaps make use of its own different regions to interact with Cyt toxins, *Bti*-Cyt1Aa and/or *Btd*-Cyt2Aa2, for their synergistic interactions.

In conclusion, we have here provided pivotal insights for the first time into the synergistic interactions between *Bti*-Cry4Ba and *Btd*-Cyt2Aa2, revealing that Cry4Ba essentially utilizes the two aromatic loop-residues, Tyr^{332} in β2–β3 loop and Phe^{364} in β4–β5 loop, for synergistically binding to its alternative receptor-Cyt2Aa2.

Acknowledgments

This work was supported in part by grants from the Thailand Research Fund (TRF) in cooperation with the Commission of Higher Education (CHE). The scholarship from CHE (to C.L.) is gratefully acknowledged.

Appendix A. Supplementary data

Supplementary data associated with this article can be found, in the online version, at http://dx.doi.org/10.1016/j.bbrc.2013.04.078.

References

[1] A. Bravo, S.S. Gill, M. Soberón, Mode of action of *Bacillus thuringiensis* Cry and Cyt toxins and their potential for insect control, Toxicon 49 (2007) 423–435.
[2] B.A. Federici, H.-W. Park, D.K. Bideshi, Overview of the basic biology of *Bacillus thuringiensis* with emphasis on genetic engineering of bacterial larvicides for mosquito control, Open Toxinol. J. 3 (2010) 83–100.
[3] C. Angsuthanasombat, Structural basis of pore formation by mosquito-larvicidal proteins from *Bacillus thuringiensis*, Open Toxinol. J. 3 (2010) 119–125.
[4] L. Regis, M.H. Silva-Filha, C. Nielsen-LeRoux, J.F. Charles, Bacteriological larvicides of dipteran disease vectors, Trends Parasitol. 17 (2001) 377–380.
[5] S. Cohen, S. Albeck, E. Ben-Dov, R. Cahan, M. Firer, A. Zaritsky, O. Dym, Cyt1Aa toxin: crystal structure reveals implications for its membrane-perforating function, J. Mol. Biol. 413 (2011) 804–814.
[6] P. Boonserm, P. Davis, D.J. Ellar, J. Li, Crystal structure of the mosquito-larvicidal toxin Cry4Ba and its biological implications, J. Mol. Biol. 348 (2005) 363–382.
[7] P. Boonserm, M. Mo, C. Angsuthanasombat, J. Lescar, Structure of the functional form of the mosquito larvicidal Cry4Aa toxin from *Bacillus thuringiensis* at a 2.8-Angstrom resolution, J. Bacteriol. 188 (2006) 3391–3401.
[8] J.D. Li, J. Carroll, D.J. Ellar, Crystal structure of insecticidal delta-endotoxin from *Bacillus thuringiensis* at 2.5 Å resolution, Nature 353 (1991) 815–821.
[9] T. Khaokhiew, C. Angsuthanasombat, C. Promptmas, Correlative effect on the toxicity of three surface-exposed loops in the receptor-binding domain of the *Bacillus thuringiensis* Cry4Ba toxin, FEMS Microbiol. Lett. 300 (2009) 139–145.
[10] T. Tuntitippawan, P. Boonserm, G. Katzenmeier, C. Angsuthanasombat, Targeted mutagenesis of loop residues in the receptor-binding domain of the *Bacillus thuringiensis* Cry4Ba toxin affects larvicidal activity, FEMS Microbiol. Lett. 242 (2005) 325–332.
[11] N. Crickmore, E.J. Bone, J.A. Williams, D.J. Ellar, Contribution of the individual components of the delta-endotoxin crystal to the mosquitocidal activity of *Bacillus thuringiensis* subsp. *israelensis*, FEMS Microbiol. Lett. 131 (1995) 249–254.
[12] B.A. Federici, H.W. Park, D.K. Bideshi, M.C. Wirth, J.J. Johnson, Recombinant bacteria for mosquito control, J. Exp. Biol. 206 (2003) 3877–3885.
[13] M.C. Wirth, Mosquito resistance to bacterial larvicidal toxins, Open Toxinol. J. 3 (2010) 101–115.
[14] M.C. Wirth, H.W. Park, W.E. Walton, B.A. Federici, Cyt1A of *Bacillus thuringiensis* delays evolution of resistance to Cry11A in the mosquito *Culex quinquefasciatus*, Appl. Environ. Microbiol. 71 (2005) 185–189.
[15] C. Pérez, L.E. Fernandez, J. Sun, J.L. Folch, S.S. Gill, M. Soberón, A. Bravo, *Bacillus thuringiensis* subsp. *israelensis* Cyt1Aa synergizes Cry11Aa toxin by functioning as a membrane-bound receptor, Proc. Natl. Acad. Sci. USA 102 (2005) 18303–18308.
[16] B. Promdonkoy, P. Promdonkoy, S. Panyim, Co-expression of *Bacillus thuringiensis* Cry4Ba and Cyt2Aa2 in *Escherichia coli* revealed high synergism against *Aedes aegypti* and *Culex quinquefasciatus* larvae, FEMS Microbiol. Lett. 252 (2005) 121–126.
[17] C. Angsuthanasombat, W. Chungjatupornchai, S. Kertbundit, P. Luxananil, C. Settasatian, P. Wilairat, S. Panyim, Cloning and expression of 130-kd mosquito-larvicidal delta-endotoxin gene of *Bacillus thuringiensis* var. *israelensis* in *Escherichia coli*, Mol. Gen. Genet. 208 (1987) 384–389.
[18] P. Chayaratanasin, S. Moonsom, S. Sakdee, U. Chaisri, G. Katzenmeier, C. Angsuthanasombat, High level of soluble expression in *Escherichia coli* and characterisation of the cloned *Bacillus thuringiensis* Cry4Ba domain III fragment, J. Biochem. Mol. Biol. 40 (2007) 58–64.
[19] S. Moonsom, U. Chaisri, W. Kasinrerk, C. Angsuthanasombat, Binding characteristics to mosquito-larval midgut proteins of the cloned domain II-III fragment from the *Bacillus thuringiensis* Cry4Ba toxin, J. Biochem. Mol. Biol. 40 (2007) 783–790.
[20] C. Angsuthanasombat, P. Uawithya, S. Leetachewa, W. Pornwiroon, P. Ounjai, T. Kerdcharoen, G. Katzenmeier, S. Panyim, *Bacillus thuringiensis* Cry4A and Cry4B mosquito-larvicidal proteins: homology-based 3D model and implications for toxin activity, J. Biochem. Mol. Biol. 37 (2004) 304–313.
[21] I. Sramala, S. Leetachewa, C. Krittanai, G. Katzenmeier, S. Panyim, C. Angsuthanasombat, Charged residue screening in helix 4 of the *Bacillus thuringiensis* Cry4B toxin reveals one critical residue for larvicidal activity, J. Biochem. Mol. Biol. Biophys. 5 (2001) 219–225.
[22] A. Thammasittirong, M. Dechklar, S. Leetachewa, K. Pootanakit, C. Angsuthanasombat, *Aedes aegypti* membrane-bound alkaline phosphatase expressed in *Escherichia coli* retains high-affinity binding for *Bacillus thuringiensis* Cry4Ba toxin, Appl. Environ. Microbiol. 77 (2011) 6836–6840.
[23] C. Pérez, C. Muñoz-Garay, L.C. Portugal, J. Sánchez, S.S. Gill, M. Soberón, A. Bravo, Bacillus thuringiensis ssp. israelensis Cyt1Aa enhances activity of Cry11Aa toxin by facilitating the formation of a pre-pore oligomeric structure, Cell. Microbiol. 9 (2007) 2931–2937.
[24] P.E. Cantón, E.Z. Zanicthe Reyes, I. Ruiz de Escudero, A. Bravo, M. Soberón, Binding of *Bacillus thuringiensis* subsp. *israelensis* Cry4Ba to Cyt1Aa has an important role in synergism, Peptides 32 (2011) 595–600.